Calculation of parity-nonconserving effects in forbidden $M1$ transitions in cesium*

David V. Neuffer† and Eugene D. Commins

Physics Department, University of California, Berkeley, California, 94720
and Materials and Molecular Research Division, Lawrence Berkeley Laboratory, Berkeley, California 94720

(Received 12 July 1977)

Calculations are presented of the $E1$ amplitude expected in forbidden $M1$ transitions of Cs if parity conservation is violated in the neutral weak e-N interaction, as proposed in a number of gauge models, including that of Weinberg and Salam. Valence electron wave functions are generated as numerical solutions of the Dirac equation in a Tietz central potential, and are used to calculate excited-state lifetimes, hfs splittings, and Stark $E1$ transition amplitudes. These are compared with experiment and are in good agreement. Contributions to the $6\,^2S_{1/2}$ g-factor anomaly and to the forbidden $6\,^2S_{1/2}$-$7\,^2S_{1/2}$ and $6\,^2S_{1/2}$-$8\,^2S_{1/2}$ transitions from relativistic effects, Breit interaction, interconfiguration interaction, and hfs mixing are calculated, and it is found that this theoretical description is not entirely adequate. The parity-nonconserving $E1$ amplitude $\mathcal{E}_{PN}$ for the $6\,^2S_{1/2}$-$7\,^2S_{1/2}$ and $6\,^2S_{1/2}$-$8\,^2S_{1/2}$ transitions is evaluated. The results $\mathcal{E}_{PN}(6S$-$7S) = i3.50\times10^{-11}\,Q_W|\mu_B|$ and $\mathcal{E}_{PN}(6S$-$8S) = i1.48\times10^{-11}Q_W|\mu_B|$ are obtained. With a measured value of the $M1$ amplitude $\mathfrak{M}_{expt}$ and the Weinberg value $Q_W = -99$, we find a circular dichroism $\delta = 1.64\times10^{-4}$ for the $6\,^2S_{1/2}$-$7\,^2S_{1/2}$ transition.

I. INTRODUCTION

Existence of a neutral, weak, parity-nonconserving electron-nucleon interaction implies that forbidden $M1$ transitions in heavy atoms, e.g., $6^2P_{1/2}-7^2P_{1/2}$ in thallium (Tl) and $6^2S_{1/2}-7^2S_{1/2}$, $6^2S_{1/2}-8^2S_{1/2}$ in cesium (Cs), should exhibit circular dichroism. In a previous paper[1] (hereafter referred to as I) we presented calculations of the atomic properties of Tl relevant to the interpretation of observations of circular dichroism in the thallium transition in terms of the Weinberg-Salam gauge field model. Here we present analogous calculations for the Cs transitions. In both cases experiments are currently underway to detect the parity-nonconserving effect.

Our approach is the one-electron central field (OECF) approximation. We find numerical solutions to the Dirac equation for the valence electron in a "Tietz" central potential[2]:

$$V(r) = -\frac{e^2(Z-1)}{r(1+\eta r)^2} - \frac{e^2}{r}\,, \tag{1}$$

where parameter η is chosen to give agreement between the observed and calculated $6^2S_{1/2}$ energies. The wave functions obtained are used to calculate fine and hyperfine structure splittings, and allowed ($E1$) transition rates and excited state lifetimes. These are compared with experimental results (see Sec. II). The $6^2S_{1/2}-7^2S_{1/2}$, $6^2S_{1/2}-8^2S_{1/2}$ $M1$ amplitudes and corrections to $g_J(6^2S^2_{1/2})$ are calculated in Sec. III and compared with experiment. Relativistic contributions to the matrix elements, as well as the "Lamb" correction and corrections due to interconfiguration interaction and hyperfine mixing, are included. We find that the present theoretical formulation of these small effects is not entirely adequate. In Sec. IV we present calculations of the parity-nonconserving $E1$ amplitudes $\mathcal{E}_{PN}(6^2S_{1/2}-7^2S_{1/2})$, $\mathcal{E}_{PN}(6^2S_{1/2}-8^2S_{1/2})$ based on the Weinberg-Salam model.[3] We find

$$\mathcal{E}_{PN}(6S-7S) = 3.50\,i\times10^{-11}Q_W|\mu_B| \tag{2}$$

and

$$\mathcal{E}_{PN}(6S-8S) = 1.48\,i\times10^{-11}Q_W|\mu_B|\,. \tag{3}$$

Here $|\mu_B| = |e\hbar/2m_ec|$ and $Q_W = (1-4\sin^2\theta_W)Z-N$, where θ_W is the "Weinberg" angle. Results (2) and (3) are somewhat smaller than earlier estimates by Bouchiat and Bouchiat[4] (see Sec. IV). Finally, in Sec. V we calculate Stark matrix elements for the transitions $6^2S_{1/2}-7^2S_{1/2}$ in an external electric field, and compare our results to earlier calculations by Bouchiat and Bouchiat,[4] and to the experimental results of Bouchiat and Pottier.[5]

II. CESIUM WAVE FUNCTIONS IN THE ONE-ELECTRON CENTRAL FIELD APPROXIMATION

A. Construction of electronic wave functions

As in I, we solve the Dirac equation for the valence electron in a centrally symmetric potential $V(r)$. The latter approximates the nucleus and 54 core electrons as a fixed charge distribution. With

$$\psi = \begin{pmatrix} \dfrac{f(r)}{r} & \chi^{\mu}_{\kappa}(\theta,\phi) \\ i\dfrac{g(r)}{r} & \chi^{\mu}_{-\kappa}(\theta,\phi) \end{pmatrix},$$

the Dirac equation reduces to the coupled radial

TABLE I. Energy levels and hyperfine splittings in Cs. (See also Fig. 1.)

State	Ionization energy (calculated) ($m_ec^2=1$)	Ionization energy (measured)[6]	Hyperfine energy splitting (calculated) GHz	Hyperfine energy splitting (observed) GHz
$6S_{1/2}$	7.62024×10^{-6}	7.62024×10^{-6}	9.212	$9.193\pm<0.001$[a]
$7S_{1/2}$	3.1232×10^{-6}	3.1229×10^{-6}	2.346	2.185 ± 0.012[b]
$8S_{1/2}$	1.7201×10^{-6}	1.7117×10^{-6}	0.935	0.876 ± 0.006[b]
$9S_{1/2}$	1.0839×10^{-6}	1.0909×10^{-6}	0.468	0.438 ± 0.008[b]
$6P_{1/2}$	4.9081×10^{-6}	4.9622×10^{-6}	1.642	$1.168\pm<0.001$[a]
$6P_{3/2}$	4.7732×10^{-6}	4.7713×10^{-6}	0.723	0.611 ± 0.006[c]
$7P_{1/2}$	2.3392×10^{-6}	2.3301×10^{-6}	0.498	$0.377\pm<0.001$[d]
$7P_{3/2}$	2.2953×10^{-6}	2.2715×10^{-6}	0.224	0.199 ± 0.001[c]
$8P_{1/2}$	1.3824×10^{-6}	1.3711×10^{-6}	0.220	
$8P_{3/2}$	1.3624×10^{-6}	1.3450×10^{-6}	0.100	0.0916 ± 0.0002[e]
$9P_{1/2}$	0.9146×10^{-6}	0.9064×10^{-6}	0.117	0.093
$9P_{3/2}$	0.9037×10^{-6}	0.8924×10^{-6}	0.054	

[a]J. Abele, M. Baumann, and W. Hartmann, Phys. Lett. A 49, 205 (1974).
[b]R. Gupta, W. Happer, L. K. Lam, and S. Svanberg, Phys. Rev. A 8, 2792 (1973).
[c]K. M. Kallas, G. Markova, G. Khvotenko, and M. Chaika, Opt. Spektrosk 19, 173 (303) (1965).
[d]D. Feiertag, A. Sahm, and G. zu Putlitz, Z. Phys. 255, 93 (1972).
[e]H. Bucka and G. von Oppen, Ann. Phys. 10, 119 (1962).
[f]P. Tsekaris, J. Farley, and R. Gupta, Fifth International Conf. on Atomic Physics, Abstract J13, 250 (1976).

equations:

$$\frac{df}{dr}=-\frac{\kappa}{r}f+[2-E-V(r)]g\,,$$
$$\frac{dg}{dr}=[E+V(r)]f+\frac{\kappa}{r}g\,. \qquad (4)$$

Our units are $\hbar=m_e=c=1$, E is the ionization energy, and other notation is defined in I. The parameter η of the potential of Eq. (1) is found to be

$$\eta=355.12\text{\AA}^{-1}=2.5914a_0^{-1} \qquad (5)$$

by requiring agreement between observed and calculated $6^2S_{1/2}$ energies. The wave functions are calculated by integrating Eqs. (4) stepwise from the nuclear radius $R_0=0.016\text{\AA}$ as described in detail in I. Table I presents calculated $S_{1/2}, P_{1/2}, P_{3/2}$ energies along with the observed values (obtained from the tables of Moore[6]).

B. Hyperfine splittings

In first-order perturbation theory the hyperfine energy is given by[7]

$$W_F=\frac{8\kappa}{4\kappa^2-1}eg_N\mu_N[F(F+1)-I(I+1)-J(J+1)]$$
$$\times\int_0^\infty\frac{f(r)g(r)\,dr}{r^2}\,. \qquad (6)$$

For ^{133}Cs (the only stable isotope), $I=\frac{7}{2}$, $g_N=5.16$,[8] leading to $F=4,3$ for $J=\frac{1}{2}$ states and $F=5,4,3,2$ for $J=\frac{3}{2}$ states. Hyperfine splittings ΔE are calculated between the highest and lowest F levels. These are related to the usual hfs interaction constants A by $\Delta E_{J=1/2}=4A_{1/2}$ and $\Delta E_{J=3/2}=12A_{3/2}$. The results are presented in Table I, and compared with experimental values. Agreement is reasonably good.

C. Allowed $E1$ transition rates

For $P_{1/2}-S_{1/2}$ and $P_{3/2}-S_{1/2}$ $E1$ transitions the Einstein A coefficient is

$$A=\tfrac{4}{9}e^2\omega^3|\langle P_J|r|S_{1/2}\rangle|^2\,. \qquad (7)$$

In Table II we present radial integrals and transition rates for $P_{1/2}-S_{1/2}$, $P_{3/2}-S_{1/2}$ transitions. These numerical values are required for computation of $\mathcal{E}_{\rm PN}$ and Stark amplitudes (Secs. IV and V).

To judge the accuracy of these transition rates, we calculate values of Cs excited state lifetimes. The lifetime of a state $|L_J\rangle$ is given by

$$T_{L_J}=\Big(\sum_{L'_{J'}}A_{|L_J\rangle\to|L'_{J'}\rangle}\Big)^{-1}\,,$$

where the sum is over all states $|L'_{J'}\rangle$ with energy less than that of $|L_J\rangle$. Table III compares available measurements of Cs lifetimes with our calculated values; agreement is, again, reasonably

TABLE II. A coefficients in Cs.

Transition	$\langle r\rangle_{fi}$ radial integral ($\lambda/2\pi$)	A coefficient (10^6 sec^{-1})
$6P_{1/2}$–$6S_{1/2}$	−861.4	37.3
$7P_{1/2}$–$6S_{1/2}$	−80.4	2.40
$8P_{1/2}$–$6S_{1/2}$	−30.8	0.582
$9P_{1/2}$–$6S_{1/2}$	−18.0	0.245
$6P_{3/2}$–$6S_{1/2}$	−846.8	41.82
$7P_{3/2}$–$6S_{1/2}$	−104.0	4.11
$8P_{3/2}$–$6S_{1/2}$	−46.6	1.34
$9P_{3/2}$–$6S_{1/2}$	−28.6	0.623
$6P_{1/2}$–$7S_{1/2}$	747.3	8.00
$7P_{1/2}$–$7S_{1/2}$	−1777.3	3.83
$8P_{1/2}$–$7S_{1/2}$	−181.8	4.39
$9P_{1/2}$–$7S_{1/2}$	−73.9	0.148
$6P_{3/2}$–$7S_{1/2}$	830.3	7.80
$7P_{3/2}$–$7S_{1/2}$	−1730.0	4.27
$8P_{3/2}$–$7S_{1/2}$	−230.3	0.729
$9P_{3/2}$–$7S_{1/2}$	−101.9	0.286
$6P_{1/2}$–$8S_{1/2}$	184.8	2.79
$7P_{1/2}$–$8S_{1/2}$	1605.4	1.54
$8P_{1/2}$–$8S_{1/2}$	−3016.4	0.883
$9P_{1/2}$–$8S_{1/2}$	−322.8	0.137
$6P_{3/2}$–$8S_{1/2}$	186.8	2.50
$7P_{3/2}$–$8S_{1/2}$	1750.9	1.47
$8P_{3/2}$–$8S_{1/2}$	−2919.4	0.983
$9P_{3/2}$–$8S_{1/2}$	−396.6	0.217

good. These lifetime calculations include calculated values of $A_{|P_J\rangle\to|D_{J'}\rangle}$.

TABLE III. Lifetimes of Cs states.

State	Measured lifetime (nsec)	Calculated lifetime (nsec)
$6P_{1/2}$	34.0 ± 0.6[a]	26.8
$6P_{3/2}$	29.7 ± 0.2[b]	23.9
$7P_{1/2}$	158 ± 5[c]	149.0
$7P_{3/2}$	135 ± 1[b]	113.0
$8P_{1/2}$	307 ± 14[d]	351.0
$8P_{3/2}$	274 ± 12[d]	270.0
$8S_{1/2}$	87 ± 9[e]	82.0

[a] J. K. Link, J. Opt. Soc. Am. 56, 1195 (1966).
[b] S. Svanberg and S. Rydberg, Z. Phys. 227, 216 (1969).
[c] D. W. Pace and J. B. Atkinson, Can. J. Phys. 53, 937 (1975).
[d] J. Marek and K. Niemax, J. Phys. B 9, L483 (1976).
[e] J. Marek, Phys. Lett. A 60, 190 (1977).

III. MAGNETIC DIPOLE TRANSITION RATES

The relativistic contribution to the $6S-7S$ or $6S-8S$ $M1$ transition amplitude is

$$\mathfrak{M}_{\rm rel}=e\int\frac{g_1(kr)}{\omega}(f_ig_f+g_if_f)\,dr\,, \qquad (8)$$

where $g_1(kr)=(\pi/2kr)^{1/2}J_{3/2}(kr)$ is a spherical Bessel function, and k and ω are the wave number and angular frequency of the absorbed photon, respectively. The formula for $nP_{1/2}-n'P_{1/2}$ $M1$ transitions (as in thallium) was derived in I and is identical to Eq. (8) except for sign. We use our OECF radial wave functions to compute the numerical results

$$\mathfrak{M}_{\rm rel}(6S-7S)=9.05\times10^{-6}|\mu_B|\,, \qquad (9)$$

$$\mathfrak{M}_{\rm rel}(6S-8S)=5.68\times10^{-6}|\mu_B|\,. \qquad (10)$$

These results and additional corrections are summarized in Table IV. The Lamb correction, discussed in I, arises from the interaction between valence electron spin and core electron orbits. For $S_{1/2}-S_{1/2}$ transitions this is given by

$$\mathfrak{M}_L=-\tfrac{1}{3}e^2\langle W\rangle\mu_B\,. \qquad (11)$$

TABLE IV. Summary of contributions to the $M1$ transition rates. The poor agreement indicates that we do not fully understand the small (10^{-4}–10^{-5}, up to fourth order) effects contributing to the $M1$ amplitudes. These do not affect the calculation of $\mathcal{E}_{\rm PN}$ since that calculation depends on large, first-order amplitudes such as $\langle E1\rangle_{SP}$ and $\psi_{s,p}(\vec{r}\to0)$. The small size of $\mathcal{E}_{\rm PN}$ is determined only by the small size of the Fermi coupling constant G.

	$6S_{1/2}$ g-factor anomaly ($g=g_e+\delta_g$)	$6S_{1/2}-7S_{1/2}$	$6S_{1/2}-8S_{1/2}$
Relativistic	$+1.75\times10^{-5}$	$+9.05\times10^{-6}$	$+5.68\times10^{-6}$
Lamb	$+6.2\times10^{-6}$	$+2.87\times10^{-6}$	$+1.78\times10^{-6}$
Interconfiguration interaction	-8.3×10^{-6}	-7.0×10^{-6}	-5.9×10^{-6}
Hyperfine mixing	···	8.36×10^{-6} $(F-F')$	4.02×10^{-6} $(F-F')$
Observed value	$-1.181\pm0.002\times10^{-4}$[a]	$-4.24\pm0.34\times10^{-5}$[b]	···

[a] P. A. Vanden Bout *et al.*, Phys. Rev. 165, 88 (1968).
[b] M. A. Bouchiat and L. Pottier, J. Phys. Lett. (Paris) 37, L-79 (1976).

Here

$$\langle W\rangle = \int_0^\infty F(r_1)\left[\int_{r_1}^\infty \rho(r_2) r_2 dr_2\right] F'(r_1) r_1^2 dr_1 ,$$

where F, F' are the nonrelativistic 6S, 7S(8S) radial wave functions, respectively, and $\rho(r_2)$ is a spherically symmetric core electron density, as in I. The "orbit-orbit" correction vanishes for $S_{1/2} - S_{1/2}$ transitions.

The relativistic and Lamb contributions to the g-factor anomaly for the $6^2S_{1/2}$ state may be computed in the same way. As previously noted by Perl[9] and by Phillips,[10] the calculation of relativistic effects leads to a g-factor anomaly which is too small and of the wrong sign when compared with experimental results. It has been suggested by a number of authors that interconfiguration interaction[4,10,11] might be responsible for the discrepancy. As discussed in I, electrostatic interaction of the outer electron with excited core states does not by itself affect $M1$ transition amplitudes or the g-factor anomaly since it mixes only those configurations which have the same total angular momentum and spin $(^2S_{1/2})$. However, in second order, spin-orbit coupling allows an admixture of different $L-S$ states (such as $^2P_{1/2}$, $^4P_{1/2}$ in Cs) which can give rise to finite contributions to $M1$ transitions or g-anomalies. Our detailed nonrelativistic calculation of this effect is similar to that presented for thallium in I, and differs only slightly from the work of Phillips.[10] The ground configuration of Cs is $1s^2 \cdots 5p^6 6s$. For first-order excited configurations, we take $1s^2 \cdots 5p^5 6s 6p$ or $1s^2 \cdots 5p^5 7s 6p$. The outer s and excited p electrons can form ^1P or ^3P states which we label by ψ_1^n, ψ_2^n, respectively (where n corresponds to the nS valence electron). Thus the perturbed 6S, 7S states are written

$$|\overline{6S}\rangle = |6S\rangle + \alpha_1\psi_1^6 + \alpha_2\psi_2^6 + \beta_1\psi_1^7 + \beta_2\psi_2^7 , \qquad (12)$$

$$|\overline{7S}\rangle = |7S\rangle + \gamma_1\psi_1^6 + \gamma_2\psi_2^6 + \delta_1\psi_1^7 + \delta_2\psi_2^7 . \qquad (13)$$

LS coupling mixes the $^2S(^1P)$ states with $^2P(^1P)$ states, and also mixes $^2S(^3P)$ states with $^2P(^3P)$ and $^4P(^3P)$ states. Thus we obtain in second order:

$$\begin{aligned}|\overline{6S}\rangle = |6S\rangle &+ \cdots + \alpha_1 A_1(^2\phi_1^6) + \alpha_2 A_2(^2\phi_3^6)\\ &+ \alpha_2 A_2'(^4\phi_3^6) + \beta_1 B_1(^2\phi_1^7)\\ &+ \beta_2 B_2(^2\phi_3^7) + \beta_2 B_2'(^4\phi_3^7) ,\end{aligned} \qquad (14)$$

$$\begin{aligned}|\overline{7S}\rangle = |7S\rangle &+ \cdots + \gamma_1 C_1(^2\phi_1^6) + \gamma_2 C_2(^2\phi_3^6)\\ &+ \gamma_2 C_2'(^4\phi_3^6) + \delta_1 D_1(^2\phi_1^7)\\ &+ \delta_2 D_2(^2\phi_3^7) + \delta_2 D_2'(^4\phi_3^7) .\end{aligned} \qquad (15)$$

The ${}^m\phi_l^n$ are ${}^mP(^lP)$ states with s-electron radial quantum number n. The A_i, B_i, C_i, D_i, are determined by the electrostatic interaction between outer electrons. The expressions for this interaction are as presented by Phillips except that we find a result $\sqrt{6}$ times larger from antisymmetrizing initial and final states. For example,

$$A_1 = (\sqrt{6}/2)(F_0 + G_1)/\Delta E , \qquad (16)$$

where F_0 and G_1 are the direct and exchange electrostatic integrals and ΔE is the perturbation energy denominator.

The second-order coefficients $\alpha_i, \beta_i, \gamma_i, \delta_i$ are determined by fine-structure matrix elements of the $5p$ electron state, as computed by Phillips. For example, $\alpha_1 = \xi/\sqrt{2}\,\Delta E$, where ξ is the spin-orbit parameter of the $5p$ hole. Our value of $\xi/\Delta E = 0.07$ calculated with OECF wave functions differs slightly from Phillips' estimate $\xi/\Delta E \cong 0.10$. The coefficients are evaluated numerically using OECF wave functions and contribute as follows to the 6S − 7S $M1$ amplitude:

$$\begin{aligned}\mathfrak{M}_{\mathrm{II}}(6S-7S) &= (\alpha_1 A_1 \gamma_1 C_1 + \beta_1 B_1 \delta_1 D_1)[g(^2P) - g(^2S)]/2\\ &+ (\alpha_2 A_2 \gamma_2 C_2 + \alpha_2 A_2' \gamma_2 C_2 + \beta_2 B_2 \delta_2 D_2 + \beta_2 B_2' \delta_2 D_2')\\ &\times [g(^4P) - g(^2S)]/2 .\end{aligned} \qquad (17)$$

The results for $\mathfrak{M}_{\mathrm{II}}(6S-7S)$ and similar corrections for the 6S − 8S $M1$ amplitude and the 6S g-factor anomaly are presented in Table IV. Similar corrections due to the $(5p^5 6p 5d)$ configuration have been calculated; however, these are smaller [~25% of that obtained from Eq. (17)]. The overall uncertainty in the interconfiguration interaction correction could be as much as a factor of 2 or

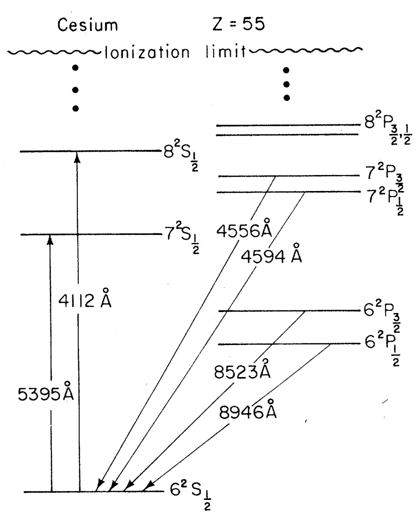

FIG. 1. Low-lying S and P levels of the Cs atom. Fine structure is enlarged and hyperfine structure is not resolved. The forbidden $M1$ transitions at 5395 and 4112 Å are shown.

3. However, as can be seen from Table IV, this calculated correction is too small to account for the observed $6S$ g factor and $6S-7S$ $M1$ amplitude by an order of magnitude. This discrepancy is not reduced much by including contributions of $5p^5n'pns$ ($n'>6$) or $5p^5n'pnd$ ($n'>6, n>s$) configurations since their contributions diminish rapidly as n, n' increase. Our conclusion, consistent with that of Phillips, is that the observed anomalies are not due to interconfiguration interaction of this type.

An appreciable correction to the $M1$ amplitude arises from hyperfine mixing. The size of this effect can be derived from Eq. (I-59), as modified for Cs $^2S_{1/2}$ states. We find

$$(\langle n'S,F|H_{\rm hfs}|6S,F\rangle - \langle 6S,F'|H_{\rm hfs}|nS,F'\rangle)\times\frac{\langle nS_{1/2},F'|M1|nS_{1/2},F\rangle}{E_{6S}-E_{nS}}. \quad (18)$$

The amplitude vanishes for $F=F'$; thus unlike the other amplitudes it only affects $F=3\rightarrow F'=4$ or $F=4\rightarrow F'=3$ transitions. The hyperfine integrals are evaluated numerically, and we employ

$$\langle nS_{1/2}F'|M1|nS_{1/2}F\rangle = -\tfrac{1}{2}e\langle F'm_F'|\vec{\sigma}|F_1m_F\rangle . \quad (19)$$

The numerical results are summarized in Table IV. An observation of the $3\rightarrow4$ and $4\rightarrow3$ transitions with the same accuracy that Bouchiat and Pottier[5] reported for the $4\rightarrow4$ and $3\rightarrow3$ components of the $6S-7S$ transitions would clearly reveal the hyperfine correction.

IV. CALCULATION OF PARITY-VIOLATING $E1$ AMPLITUDE

According to the Weinberg-Salam model, the parity-nonconserving electron-nucleus interaction provides the following interaction matrix element (I-64):

$$\langle\psi_1|H_{\rm PN}|\psi_2\rangle = -\frac{GQ_W}{2\sqrt{2}}\psi_1^\dagger(\vec{x})\gamma_5\psi_2(\vec{x})\Big|_{(\vec{x}=0)} . \quad (20)$$

This mixes S states with opposite parity P states, as follows:

$$|\overline{n}\overline{S}_{1/2}\rangle = |nS_{1/2}\rangle + \sum_{n'}\frac{\langle n'P_{1/2}|H_{\rm PN}|nS_{1/2}\rangle}{E_{nS}-E_{n'P}}|n'P_{1/2}\rangle . \quad (21)$$

TABLE V. Calculation of $\mathcal{E}_{\rm PN}$ for the $6S_{1/2}-7S_{1/2}$ transition.

Intermediate P state	$\frac{e}{3}\frac{\langle 7S\|r\|nP_{1/2}\rangle\langle nP_{1/2}\|H_{\rm PN}\|6S\rangle}{E_{6S}-E_{nP}}$	$\frac{e}{3}\frac{\langle 7S\|H_{\rm PN}\|nP_{1/2}\rangle\langle nP_{1/2}\|r\|6S\rangle}{E_{7S}-E_{nP}}$
Method 1:		
$\|6P\rangle$	$-i7.823\times10^{-11}Q_W\|\mu_B\|$	$+i6.912$
$\|7P\rangle$	$+i5.259$	$-i0.809$
$\|8P\rangle$	$+i0.303$	$-i0.093$
$\|9P\rangle$	$+i0.084$	$-i0.031$
Total	$-i2.18$	$+i5.98$
	$=i3.80\times10^{-11}Q_W\|\mu_B\|$	
Method 2:		
	$-i1.75$	$+i5.24$
	$=i3.50\times10^{-11}Q_W\|\mu_B\|$	

Calculation of $\mathcal{E}_{\rm PN}$ for the $6S_{1/2}\rightarrow8S_{1/2}$ transition

Intermediate P state	$\frac{e}{3}\frac{\langle 8S\|r\|nP_{1/2}\rangle\langle nP_{1/2}\|H_{\rm PN}\|6S\rangle}{E_{6S}-E_{nP}}$	$\frac{e}{3}\frac{\langle 8S\|H_{\rm PN}\|nP_{1/2}\rangle\langle nP_{1/2}\|r\|6S\rangle}{E_{8S}-E_{nP}}$
Method 1:		
$\|6P\rangle$	$-i1.935\times10^{-11}Q_W\|\mu_B\|$	$+i2.445$
$\|7P\rangle$	$-i4.751$	$+i0.647$
$\|8P\rangle$	$+i5.027$	$-i0.303$
$\|9P\rangle$	$+i0.366$	$-i0.054$
Total	$-i1.29$	$+i2.74$
	$=i1.44\times10^{-11}Q_W\|\mu_B\|$	
Method 2:		
	$-i0.81$	$+i2.29$
	$=i1.48\times10^{-11}Q_W\|\mu_B\|$	

Thus Eq. (20) can be reduced to

$$\langle n'P_{1/2}|H_{PN}|nS_{1/2}\rangle = i\,\frac{GQ_W}{8\sqrt{2}\pi}(f_p g_s - f_s g_p)\bigg|_{r=0}\delta_{m_s m_p}. \quad (22)$$

The $r=0$ symbol indicates that the expression is averaged over the nuclear volume, and we assumed a constant nucleon density for $r<0.016\lambda\!\!\!^{-}$. An alternative procedure would be to assume a pointlike nucleus and evaluate $\langle H_{PN}\rangle$ at the nuclear radius; this produces a value 2% larger.

An $E1$ transition amplitude is now possible between the perturbed S states. Its value is given by

$$\mathcal{E}_{PN} = \langle \overline{nS}_{1/2}|E1|\overline{6S}_{1/2}\rangle = \sum_{n'}\left(\langle nS_{1/2}|E1|n'P_{1/2}\rangle\frac{\langle n'P_{1/2}|H_{PN}|6S_{1/2}\rangle}{E_{6S}-E_{n'}} + \frac{\langle nS_{1/2}|H_{PN}|n'P_{1/2}\rangle}{E_{nS}-E_{n'}}\langle n'P_{1/2}|E1|6S_{1/2}\rangle\right), \quad (23)$$

where

$$\langle nS_{1/2}|E1|n'P_{1/2}\rangle = e\langle nS_{1/2}|\vec{\epsilon}\cdot\vec{r}|n'P_{1/2}\rangle \cong \frac{e}{3}\int f_s r f_p\,dr \quad (24)$$

and the last expression is derived for the particular case $m_s = m_p = -\frac{1}{2}$, $\vec{\epsilon} = \hat{e}_z$. The numerical results are summarized in Table V, where Eq. (23) has been evaluated by two methods: (1) A finite sum over the nearest four intermediate p states; (2) The use of the Dirac Green's function. The Green's function automatically includes all intermediate states, including continuum and autoionizing states as shown in I. The two methods give similar results, as shown in Table V. The Green's function method is considered more accurate, since it is more complete.

In the Weinberg model, with $\sin^2\theta_W = 0.30$ as suggested by the experiment of Reines *et al.*,[12]

$$Q_W = -[(4\sin^2\theta_W - 1)Z + N] = -99 \quad (25)$$

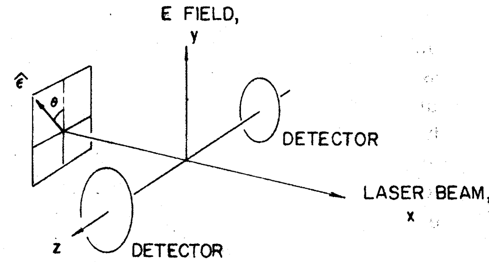

FIG. 2. Coordinate system and orientations of electric field $\vec{E}$, photon beam, and polarization. Detectors are placed as in the experiment on Tl of Chu *et al.* (Ref. 13).

for ^{133}Cs. This leads to a value of $\mathcal{E}_{PN} = -i3.47\times10^{-9}|\mu_B|$ for the $6S_{1/2}-7S_{1/2}$ transition. This corresponds to a circular polarization (circular dichroism) of

$$\delta = \frac{2\,\mathrm{Im}(\mathcal{E}_{PN})}{\mathfrak{M}_{exp}} = 1.64\times10^{-4}. \quad (26)$$

Bouchiat and Bouchiat,[4] using nonrelativistic wave functions with a relativistic correction factor for $\langle H_{PN}\rangle$, a modified Bates-Damgaard method for $e\langle\vec{\epsilon}\cdot\vec{r}\rangle$, and a finite sum over the nearest four P states, obtained a somewhat higher estimate of $-i4.7\times10^{-9}|\mu_B|$ for $\mathcal{E}_{PN}$ in this transition, and a similarly higher result for the $6S-8S$ transition.

Using our analysis of hyperfine structure and excited states decay rates, we can form an estimate of errors. Our hyperfine structure and fine structure calculations indicate that the magnitudes of the P-state wave functions as $r\to0$ are ~10% lower than physically accurate. However, decay rate comparisons indicate that our $\langle E1\rangle$ matrix elements are too large by ~10%. These errors cancel in the evaluation of $\mathcal{E}_{PN}$ and our $\mathcal{E}_{PN}$ error should not be greater than ~10%.

V. CALCULATION OF THE STARK EFFECT $E1$ TRANSITIONS

In actual experimental practice (see Bouchiat and Pottier) $\mathfrak{M}$ and $\mathcal{E}_{PN}$ are measured in interference with the $E1$ transition induced by an external electric field. $\mathfrak{M}$ and $\mathcal{E}_{PN}$ are not directly measured

TABLE VI. Stark effect $E1$ amplitudes.

A. $\langle\overline{7S}\|E1\|\overline{6S}\rangle$	$e^2\alpha$ $[10^{-5}\|\mu_B\|\ (\mathrm{V/cm})^{-1}]$	$e^2\beta$ $[10^{-6}\|\mu_B\|\ (\mathrm{V/cm})^{-1}]$	$\left\|\frac{\alpha}{\beta}\right\|$
Finite sum method:	−2.043	−1.78	11.5
Green's function:	−1.972	−1.96	10.06
Experimental value:	···	···	8.8 ± 0.4
B. $\langle\overline{8S}\|E1\|\overline{6S}\rangle$			
Finite sum method:	−3.132	−3.71	8.45
Green's function:	−3.166	−3.97	7.86

but are compared to the induced Stark effect amplitude $\mathcal{E}_S$, which is calculated. Therefore, it is important to calculate a reliable value of $\mathcal{E}_S$.

The coordinate system used in the calculation is illustrated in Fig. 2, and is the same used in I. An electric field $E_0\hat{e}_y$ is perpendicular to the photon propagation vector $\hat{e}_x$. The photon has polarization $\vec{\epsilon} = \cos\theta\hat{e}_y + \sin\theta\hat{e}_z$, and the ${}^2S_{1/2}$ states are mixed with $P_{1/2}, P_{3/2}$ states by Stark effect.

$$|\overline{nS_{1/2}}\rangle = |nS_{1/2}\rangle + \sum_{n'P_{1/2}} \frac{\langle n'P_{1/2}|e\vec{E}_0\cdot\vec{r}|nS_{1/2}\rangle}{\Delta E_{1/2}} |n'P_{1/2}\rangle + \sum_{n'P_{1/2}} \frac{\langle n'P_{3/2}|e\vec{E}_0\cdot\vec{r}|nS_{1/2}\rangle}{\Delta E_{3/2}} |n'P_{3/2}\rangle . \quad (27)$$

There is an $E1$ transition amplitude $\mathcal{E}_S$ between the perturbed states, which we represent as a 2×2 matrix whose rows and columns are labeled by $m_J(6S_{1/2})$ and $m_J(nS_{1/2})$, respectively,

$$\mathcal{E}_S = \langle\overline{nS_{1/2}}|e\hat{\epsilon}\cdot\vec{r}|\overline{6S_{1/2}}\rangle = e^2E_0 .$$

$m_J(7S_{1/2})$ \ $m_J(6S_{1/2})$	$\frac{1}{2}$	$-\frac{1}{2}$
$\frac{1}{2}$	$\alpha\cos\theta$	$-i\beta\sin\theta$
$-\frac{1}{2}$	$-i\beta\sin\theta$	$\alpha\cos\theta$

(28)

$$\alpha = \frac{1}{9}\sum_{n'P_{1/2}} R_{nS,n'P_{1/2}} R_{6S,n'P_{1/2}} \times\left(\frac{1}{E_n - E_{n'P_{1/2}}} + \frac{1}{E_6 - E_{n'P_{1/2}}}\right) + \frac{2}{9}\sum_{n'P_{3/2}} R_{nS,n'P_{3/2}} R_{6S,n'P_{3/2}} \times\left(\frac{1}{E_6 - E_{n'P_{3/2}}} + \frac{1}{E_n - E_{n'P_{3/2}}}\right) , \quad (29)$$

$$\beta = \frac{1}{9}\sum_{n'P_{1/2}} R_{nS,n'P_{1/2}} R_{6S,n'P_{1/2}} \times\left(\frac{1}{E_6 - E_{n'P_{1/2}}} - \frac{1}{E_n - E_{n'P_{1/2}}}\right) + \frac{1}{9}\sum_{n'P_{3/2}} R_{nS,n'P_{3/2}} R_{6S,n'P_{3/2}} \times\left(\frac{1}{E_n - E_{n'P_{3/2}}} - \frac{1}{E_6 - E_{n'P_{3/2}}}\right) , \quad (30)$$

TABLE VII. $n^2S_{1/2}$-$6^2S_{1/2}$ transition amplitudes: $\langle\overline{nS}|E1+M1|\overline{6S}\rangle$. $\vec{\epsilon} = \hat{e}_y\cos\theta + \hat{e}_z\sin\theta$, $\alpha' = e^2\alpha E_y$, $\beta' = e^2\beta E_z$.

$m_z(nS_{1/2})$ \ $m_z(6^2S_{1/2})$	$+\frac{1}{2}$	$-\frac{1}{2}$
$+\frac{1}{2}$	$\alpha'\cos\theta$ $+\mathfrak{M}\cos\theta$ $-\mathcal{E}_{PN}\sin\theta$	$-i\beta'\sin\theta$ $+i\mathfrak{M}\sin\theta$ $+i\mathcal{E}_{PN}\cos\theta$
$-\frac{1}{2}$	$-i\beta'\sin\theta$ $-i\mathfrak{M}\sin\theta$ $-i\mathcal{E}_{PN}\cos\theta$	$\alpha'\cos\theta$ $-\mathfrak{M}\cos\theta$ $+\mathcal{E}_{PN}\sin\theta$

where

$$R_{6S,n'P_{1/2}} = \langle 6S_{1/2}|r|n'P_{1/2}\rangle, \quad E_6 = E(6S_{1/2}) , \quad (31)$$

etc. The quantities α and β have been evaluated by summation over the nearest $P_{1/2}, P_{3/2}$ states, and also by use of the Green's function. The results are summarized in Table VI.

Our results can be compared with the calculation of Bouchiat and Bouchiat, which was used in the experimental determination of $\mathfrak{M}(6S\to 7S)$.[5] Their calculation used the $E1$ oscillator strengths calculated by Stone and they determined signs by the Bates-Damgaard method and summed over the four lowest energy levels. Their value is $e^2\alpha = -1.62\times10^{-5}|\mu_B|$ $(\text{V/cm})^{-1}$ and $|\alpha/\beta| \cong 7.0$ for $\mathcal{E}_S(7S-6S)$. Our value of $|\alpha/\beta|$ is 10.1 and agrees more closely with the experimental result 8.8 ±0.4. However, our analysis of excited-state lifetimes leads us to suspect that our value $e^2\alpha = -1.97 \times10^{-5}|\mu_B|$ $(\text{V/cm})^{-1}$ is ~10% to 20% too large, so the true value of $e^2\alpha$ is probably somewhere between our result and that of Bouchiat and Bouchiat.

In Table VII we combine the calculations of $\mathcal{E}_S$, $\mathfrak{M}$, and $\mathcal{E}_{PN}$ in a single 2×2 matrix so that the interference among these amplitudes can be readily extracted. Table VII gives the $(6S\to nS)$ transition amplitudes with the photon directed along $\hat{e}_x$ with polarization $\vec{\epsilon} = \vec{e}_y\cos\theta + \vec{e}_z\sin\theta$.

We thank Professor Charles Schwartz and Dr. Peter Mohr for numerous useful discussions.

*Research supported by the U. S. Energy Research and Development Administration.

†Current address: Theoretical Physics Group, Lawrence Berkeley Laboratory, Berkeley, Calif. 94720.

[1]D. V. Neuffer and E. D. Commins, Phys. Rev. A 16, 844 (1977).

[2]T. Tietz, J. Chem. Phys. 22, 2094 (1954).

[3]S. Weinberg, Phys. Rev. Lett. 19, 1264 (1967); A. Salam, in *Elementary Particle Theory*, edited by N. Svartholm (Alquist and Vorlag, Stockholm, 1968).

[4]M. A. Bouchiat and C. Bouchiat, Phys. Lett. B 48, 111 (1974); J. Phys. (Paris) 35, 899 (1974); 36, 493 (1975).
[5]M. A. Bouchiat and L. Pottier, J. Phys. Lett. (Paris) 37, L-79 (1976).
[6]C. E. Moore, Atomic Energy Levels, Vol. III, Circular of Natl. Bur. of Stand. 467 (1958).
[7]M. E. Rose, *Relativistic Electron Theory* (Wiley, New York, 1961).
[8]C. M. Lederer, J. M. Hollander, and I. Perlman, *Table of Isotopes* (Wiley, New York, 1967).
[9]W. Perl, Phys. Rev. 91, 852 (1953).
[10]M. Phillips, Phys. Rev. 88, 202 (1952).
[11]I. B. Khriplovich, Sov. J. Nucl. Phys. 21, 538 (1975) [Yad. Fiz. 21, 1046 (1975)].
[12]F. Reines *et al.*, Phys. Rev. Lett. 37, 315 (1976).
[13]S. Chu, R. Conti, and E. D. Commins, Phys. Lett. A 60, 96 (1977).